

Design and FEM analysis of high-power density C-core permanent magnet transverse flux generator with reduced PM volume

Ali Muhammad¹ | Faisal Khan¹ | Basharat Ullah¹  | Ahmad H. Milyani^{2,3} | Abdullah A. Azhari⁴

¹Department of Electrical and Computer Engineering, COMSATS Institute of Information Technology, Abbottabad, Pakistan

²Department of Electrical and Computer Engineering, King Abdulaziz University, Jeddah, Saudi Arabia

³Center of Research Excellence in Renewable Energy and Power Systems, King Abdulaziz University, Jeddah, Saudi Arabia

⁴The Applied College, King Abdulaziz University, Jeddah, Saudi Arabia

Correspondence

Department of Electrical and Computer Engineering, COMSATS Institute of Information Technology, Abbottabad 22060, Pakistan.
Email: alimuhammad@cuiatd.edu.pk

Abstract

Transverse flux machines are made up of armature coils wound in a circular direction and surrounded by armature cores. This configuration enables machines to be designed for multi-pole structures while maintaining a simple coil geometry regardless of the pole count. As a result, these machines generate more torque and power density than most of the machines with windings wound around teeth and inserted into slots. However, transverse flux machines continue to face manufacturing difficulties because a large number of relatively small permanent magnets are required. Thus, a permanent magnet transverse flux generator (PMTFG) is designed with half the magnets on the rotor in comparison with a regular design while generating 18% better power density at the same size and excitation conditions. After proper parameter selection, the electromagnetic performance of the design is examined, and the viability of the design is verified using a three-dimensional finite-element model (FEM). Further analyses were carried out to examine the effect of stator core material and air gap length on the performance of PMTFG. Furthermore, a prototype of the proposed topology is built, which validates the performance obtained through FEM.

1 | INTRODUCTION

Permanent magnet transverse flux machines (PMTFM) have unique advantages in terms of high torque and power density. Since there is no gearbox between the electric machine and the prime mover or load in direct-drive systems, PMTFMs are particularly well suited for usage in these types of power systems. The use of TFMs in variable speed wind turbines and in-wheel traction appears to have much potential [1].

In a variety of areas, numerous PMTFMs with interesting novelties have been developed and studied [2]. It has been suggested to use flux-concentrated PMTFM to attain high torque or power densities [3]. For the purpose of minimizing flux leakage and weight of the machine, a unique double-coil PMTFM has been presented [4]. An innovative solution to the losses caused by inactive magnets is described in [5], which makes use

of a fall-back path for the rotor. The fall-back rotor path acts as a flux return path in the absence of active magnets, which increases the weight and iron losses of the machine. A novel PMTFM [6] uses the circumferential flux path in the additional rotor core to produce 3D flux paths. This permits laminations to construct the stator claw poles, eliminating SMC's disadvantages, but adding a rotor makes the mechanical system more complex and expensive. A new architecture of TFPMM with novel SMC cores is presented in [7]; it employs low-cost ferrite magnets and high-fill-factor ring winding. By putting a lot of low-cost ferrite magnets between the stator poles, this design is complicated and bulky.

Since the stator in a PMTFM is made up of magnetic cores, the space for the armature windings can be increased without compromising the available space for the main magnetic flux. For the PMTFM, numerous magnetic cores have

been studied. The U-shaped structure has surface-mounted PMs. The axial rotation of the U-cores forms the transverse flux plane of the magnetic flux. Some modification in the traditional U-cores are presented in [4]. Due to structure similarities, both U- and C-cores are sometimes referred to by the same name in the literature. U-cores guide magnetic flux in the axial plane of PMTFM with surface-mounted PMs, whereas C-cores guide flux over a skewed line in PMTFM with flux-concentrating PMs. C-core PMTFMs have fewer losses and higher torque but are harder to make [8]. The claw-pole PMTFM has higher torque densities and is lighter than radial and mutual flux path machines of the same volume. If magnet mass is restricted instead of outer volume, claw-pole PMTFM torque capability is reduced [9]. The SMC-dependent manufacturing process is troublesome, although assembly is easier than previous PMTFMs [10]. A double-sided machine with two passive rotors is made possible by the H-core in the stator [11]. The E-core increases torque density and magnet utilization by shortening the flux path with cross-leg pole windings. E-cores with ring windings create a double-sided stator [12].

PMTFM cogging torque is a major issue that is affecting its performance. PMTFMs often have larger cogging torque as compared to other PM machines. This is because the rotor has double the poles of the stator [13]. For the specific design of a PMTFG, the procedures mentioned in the literature for skewing the stator poles or PMs on the rotor for one-pole pitch are inapplicable [14]. Significant research on improving PMTFM concerning cogging torque is available in [15, 16]. A parametric analysis using a single-phase PMTFM to find the best air gap size and reduce cogging torque is presented in [17]. A potential strategy for lessening PMTFM's cogging torque is investigated in [18]. The cogging torque reduction is accomplished through the utilization of three different stator step-skewed configurations, namely a three-step-skewed stator, a two-step-skewed stator, and a one-step-skewed stator.

Magnet utilization is one of the shortcomings of PMTFM over other types of PM machines. In PMTFM, only half of the magnets are facing the stator magnetic poles at any given moment, establishing a flux linkage. The primary flux is partially cancelled by nearby magnets with opposite polarity (inactive magnets) [19]. However, [20] offers an approach in which all of the magnets are used in conjunction with additional alternating stator cores. This has an impact on the power-to-weight ratio, raises the machine's cost, and complicates the production process.

Given the manufacturing problems in PMTFM, [21] developed a PMTFG with fewer PMs on the rotor as provided in [22] and depicted in Figure 1. The study in [21] is further extended here, and the number of rotor PMs and stator cores are further reduced to 16 and 8, respectively, lowering the machine's overall cost. To validate the proposed 8/16 PMTFG, a prototype is built here. The key addition to this article is the use of a double armature coil in the stator, utilizing the free space in stator C-cores having pole shoes. The rotor consists of PMs, which are enclosed in an aluminum housing, which simplifies production.

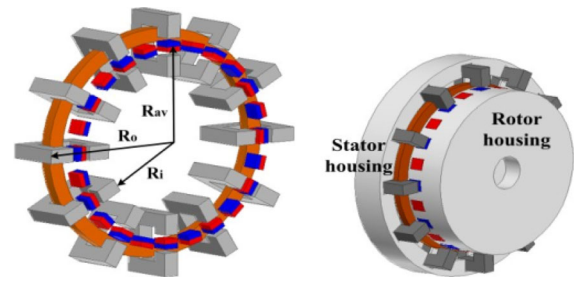


FIGURE 1 Design of state-of-the-art PMTFG

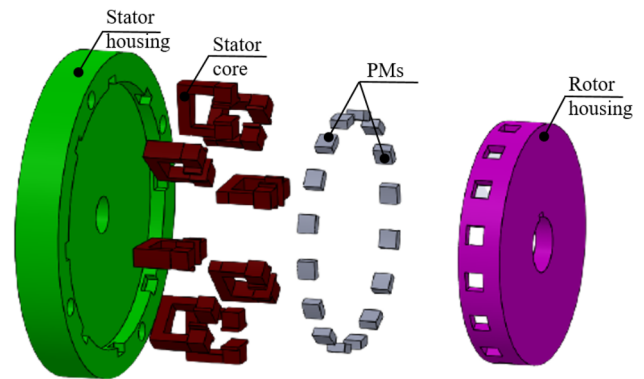


FIGURE 2 Schematic of the presented PMTFG

2 | DESIGN AND PARAMETER SELECTION

2.1 | Design of a proposed model

A proposed design of single-phase PMTFG consisting of a semi-closed stator and a surface-mounted PM rotor is shown in Figure 2, and Table 1 has a list of the parameters. The proposed design uses an aluminium casing for the rotor in which PMs are housed on a surface perpendicular to the stator C-cores. In a single-sided PMTFG, the number of stator pole pairs is always equal to half the number of rotor PM pole pairs. The stator, in this case, is made out of C-cores, which are semi-closed in shape and pole-shoe to improve flux catching capability. The aluminium casing serves as the support and houses the rotor PMs and stator cores. Ring winding is used in a stator, wound circumferentially around the slots of the stator cores, thereby generating a single coil with several turns. To utilize the feasible space in the core and make the machine fault-tolerant, double coils are used.

2.2 | Parameter selection

The PMTFM is noted for its high torque and power density in literature. Its proper selection of parameters like stator cores, rotor pole number, air gap length, and armature winding can boost the power rating. The selection of configuration and design parameters of the machine are calculated as follows.

TABLE 1 Specifications for designed models

Parameters	Value
Pole pairs, P	6/8/10/12
No. of PMs, M	12/16/20/24
Frequency, f	150 Hz/250 Hz/200 Hz/300 Hz
Rated speed, n_r	1500 rpm
Turns per Coil, N	90
Outer radius, R_0	155 mm
Shaft radius, R_s	97 mm
Air gap, g	1 mm
Length of magnet, l_m	10 mm
Width of PM, w_m	10 mm
Height of PM, h_m	5 mm
Width of C-core, w_c	14 mm
Total length of C-core, l_c	30 mm
Width of pole, l_p	10 mm
Height of pole, l	3.5 mm
Length of C-core, $b_s + b_0$	14.5 mm
Yoke height, h_y	8 mm
Arc of pole-shoe, P_f	16 mm
PM material	Neomax (N35)
Stator core material	Steel

2.2.1 | Core pole study

The PMTFM's primary and most prominent advantage is its capability to produce high power and torque density. Flux density B_0 in the air gap of the TFFPM machine can be stated as [23]:

$$B_0 = \frac{B_r}{1 + \frac{g}{b_M}}. \quad (1)$$

Here, B_r shows the remanence induction of the PM, b_M is the magnet's thickness, and g is the length of the air gap. This means that the magnetic loading can be increased simply by increasing the number of pole pairs rather than modifying the armature ampere-turns or machine diameter. The PMTFM makes use of this effect to generate high specific torque density. However, this can increase the machine's weight, cost, and total core losses. Furthermore, the high pole number reduces the machine's efficiency by increasing core losses. As a result, selecting the ideal pole number for the machine's best performance in a certain application is required. Besides this, increasing ampere-turns in stator winding by using the viable space of a semi-closed stator core can improve the machine's performance as both electric and magnetic loading are decoupled. As given in the equation [23]:

$$E = k_f N \phi \frac{\Omega}{2\tau}, \quad (2)$$

where E is the EMF, k_f represents the waveform factor, N shows the coil turns, ϕ represents the flux across the winding, Ω is the mover's mechanical speed, and τ is the pole pitch.

2.2.2 | Air gap length

The length of air gap is identified as a critical factor in the design process of electrical machines. The narrower air gap is enhanced by providing a low reluctance path that increases performance. However, in terms of manufacturing tolerance and high-precision machining, it comes at a cost. A large air gap is not as detrimental on a surface-mounted rotor because the PMs act as an extra air gap for the flux coming from the stator, needing it to pass through both the mechanical and radial air gaps. A narrow air gap becomes more important when the flux concentration is high. The air gap's length affects several PMTFM features. Compared to the PM radial flux machine (PMRFM), the PMTFM is more reliant on the air gap. However, the mechanical design of such machines, as well as the conversion needs, should be considered. Considering the aforesaid points, the air gap effect on the performance of the generator is carried out for the proposed design, and an efficient air gap length, that is, of 1 mm is selected for the final design.

2.2.3 | Number of armature coils

In PMTFM, two types of armature winding configuration are utilized, that is, ring winding and pole winding. In ring winding, a simple ring is placed in the stator C-core of PMTFM while pole winding is wound across each leg of E or C-core. The manufacturing is easier with a ring winding structure since it allows for a higher filling factor and less copper weight, so ring winding is selected for the proposed design. To increase the flux linkage and back-EMF, PMTFG with a double armature coil and pole shoe is proposed for the selected rotor pole and stator core number.

3 | PERFORMANCE ANALYSIS

The optimal combination of stator C-cores and rotor poles for efficient performance in a PMTFG with 6/12, 8/16, 10/20, and 12/24 poles are examined. The preliminary results of the analysis are used to determine the optimal core-pole configuration for maximising back EMF and power performance. No-load and load analysis are the two main parts of the investigation. In an open-circuit study, the effects of rotor PM on the flux linkage, flux distribution, back EMF, and cogging torque are investigated. In load analysis, variables such as resistive load current, losses, power, efficiency, and power density are studied. The flowchart for performance analysis is depicted in Figure 3.

The single- and double-coil configurations for all designed core pole studies are shown in Figures 4 and 5, respectively. This includes the 12/24, 10/20, 8/16, and 6/12 models. The detailed dimensions are given in Figure 6. The C-core stator holds the

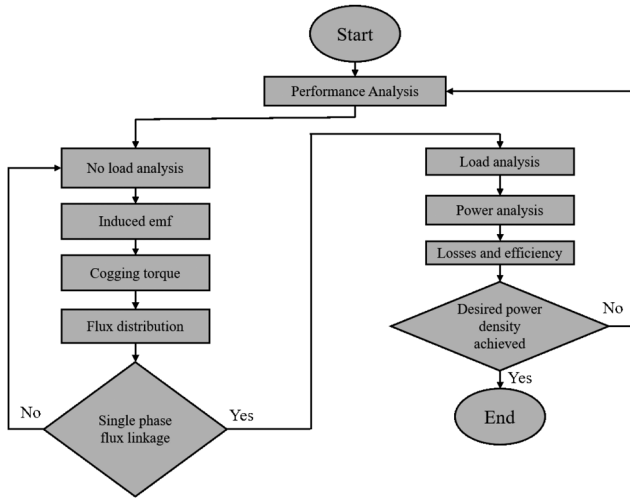


FIGURE 3 Performance analysis flow chart

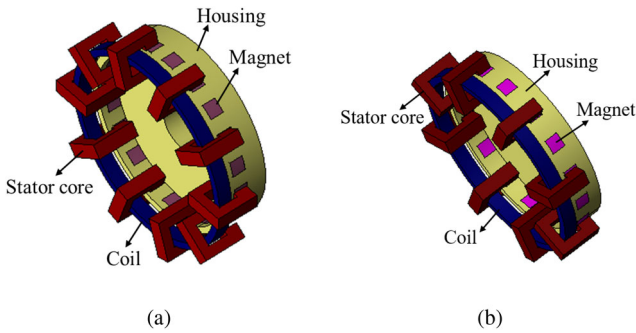


FIGURE 4 PMTFG with single-coil having (a) 10/20 cores/PMs and (b) 8/16 cores/PMs

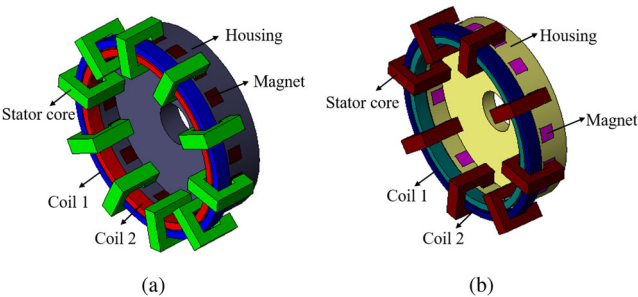


FIGURE 5 PMTFG with double-coil having (a) 10/20 cores/PMs and (b) 8/16 cores/PMs

two ring-shaped coils. Because the polarity of the PMs changes as the machine’s rotor rotates, the magnetic field’s path changes. In both coils, an alternating voltage is induced.

3.1 | FEM simulation analysis

This part presents 3D-FEM findings for single and double coil 8/16, 10/20, and 12/24 models. Geometry for 3D-FEM

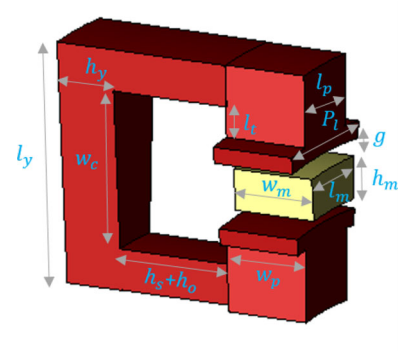


FIGURE 6 Detailed dimensions of presented PMTFG

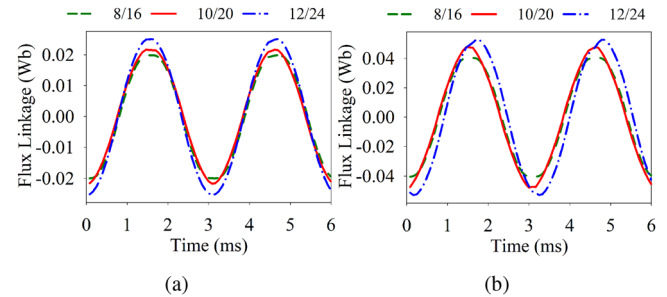


FIGURE 7 Open circuit flux linkage of the presented PMTFG @ 1500 rpm: (a) single-coil and (b) double-coil

analysis is created in multi-physics software, and the resulting model is analyzed in JMAG-Designer v20.1. Both load and no-load characteristics are taken into account while calculating performance metrics.

3.1.1 | Open circuit performance of PMTFG

All designed PMTFG models undergo open circuit analysis, including flux linkage and distribution, induced EMF, and cogging torque. Figure 7a shows the flux linkage of PMTFG designs with the single-coil arrangement, and Figure 7b illustrates the flux linkage with a double coil configuration at 1500 rpm. Despite the fact that the flux linkage in 10/20 PMTFG falls with a single armature coil, increasing the number of stator winding coils significantly improved the flux linkage. The induced EMF can be found by using Equation (3):

$$Induced E.M.F = -N \frac{d\phi}{dt}, \tag{3}$$

where N represents the total number of turns in a coil and d/dt represents the flux linkage rate of change. Figure 8a depicts the waveform of the induced voltage for single-coil PMTFG models, whereas Figure 8b displays the induced voltage waveform of PMTFG models with double coil design at rated speed (1500 rpm) by using 3D-FEA. The induced voltage is found to have a nearly sinusoidal waveform with small harmonics. In the case of double-coil PMTFG, the research indicates that doubling the

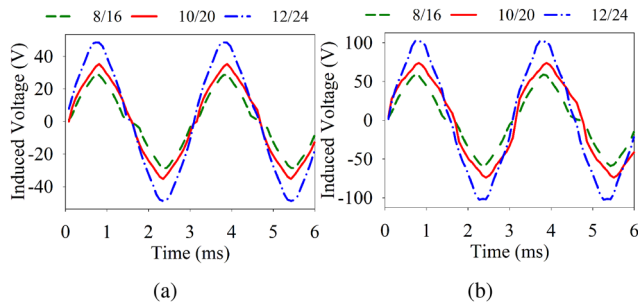


FIGURE 8 Induced-EMF of the presented PMTFG @ 1500 rpm: (a) single-coil and (b) double-coil

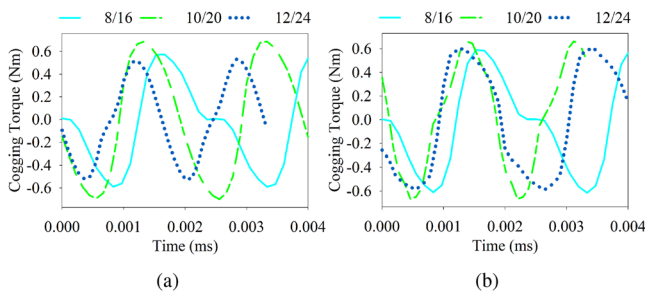


FIGURE 9 Cogging torque of the presented PMTFG: (a) single-coil and (b) double-coil

stator winding coils increases the induced voltage by a factor of two. Cogging torque of the PMTFG is a matter of concern that affects the generator’s performance. As the number of rotor poles is double that of stator poles, the circumferential distance between magnets increases, and PMTFG has a higher cogging torque than other types. As a result, 10/20 PMTFG has the highest cogging torque among all the designed models. For single and double-coil designs, cogging torque is plotted in Figure 9.

3.1.2 | Generator performance of PMTFG

The performance of three simulated models is evaluated under various load conditions. Iron losses, input power, output power, efficiency, and power density are simulated and analyzed. The iron and copper losses of all the simulated designs are provided in Figure 10. The iron losses shown in Figure 10a stays the same in single and double-coil configuration while the copper losses shown in Figure 10b get doubled in the double-coil configuration. For all types, Figure 11 shows the generator’s efficiency at varied loads. The graph illustrates that the double coil 8/16 PMTFG is more efficient than other variants. As the number of stator cores decreases, iron losses decrease, and back EMF improves with a double stator winding coil. However, when another coil is added to the 12/24 PMTFG, the back EMF increases but not the efficiency because copper losses increases while core losses remain the same. The output power (P_o) is calculated using the requisite rating voltage (V_r), number of phases

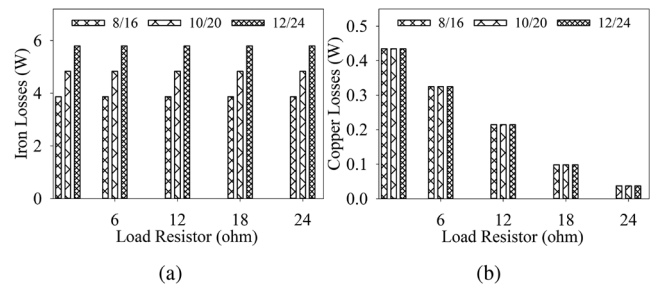


FIGURE 10 Losses of the presented PMTFG: (a) iron losses and (b) single-coil copper losses

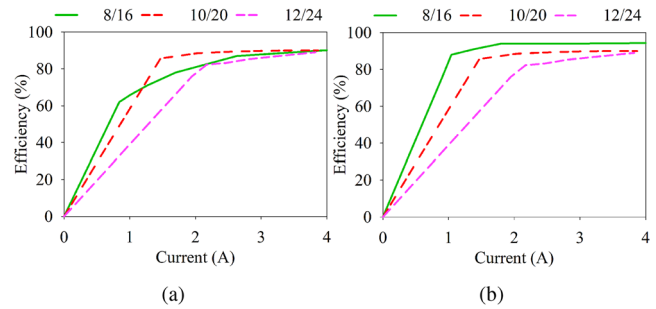


FIGURE 11 Relation of output current and efficiency of the presented PMTFG: (a) single-coil and (b) double-coil

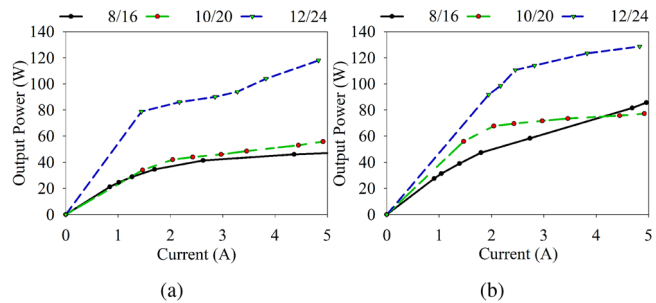


FIGURE 12 Relation of output current and P_o of the presented PMTFG: (a) single-coil and (b) double-coil

(m), phase current (I_r), efficiency (η), and power factor:

$$P_o = mV_r I_r \eta \cos(\Theta). \tag{4}$$

Figure 12 displays the output power for all designed models of PMTFG with both topologies at various load currents, demonstrating that as the load current increases, the output power also increases. The 12/24 PMTFG provides the highest output power of all other PMTFG types using the double stator coil. Figure 13a shows the efficiency compared to output power for single armature coil models, and Figure 13b shows the efficiency compared to output power for double armature coil models. The 10/20 PMTFG is more efficient in all single armature coil models, whereas the 8/16 has high efficiency in double armature coil models since the double use of the stator coil improves induced voltage.

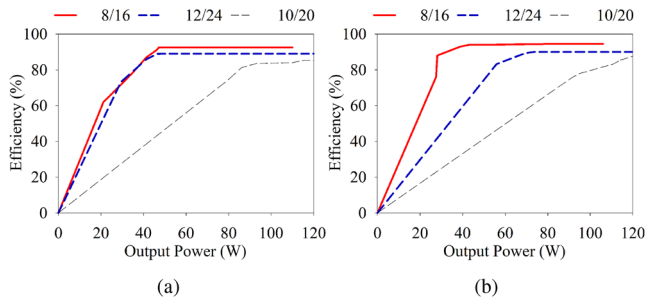


FIGURE 13 Relation of P_o and efficiency of the presented PMTFG: (a) single-coil and (b) double-coil

4 | EFFICIENT DESIGN SELECTION

One design is selected among all simulated models for further analysis and fabrication based on performance superiority over conventional one to achieve the desired objectives. Out of all the simulated models, the double coil 8/16 PMTFG is chosen because:

- Double coil configuration improves the electromagnetic flux of the generator that in turn increases back EMF.
- Double coil configuration makes the generator fault tolerant.
- Reduced stator C-cores minimize iron losses, weight, and cost of the generator.
- Reduced PM rotors decrease both weight and overall cost.
- It gives better efficiency and power density as compared to the other model.

5 | FURTHER ANALYSIS OF EFFICIENT DESIGN

Further analyses are carried out on efficient design to see the effect of air gap length and stator core materials.

5.1 | Effect of air gap length

The air gap length is an important consideration in the design of electrical machines. A short pole pitch is usually required to generate the highest possible no-load voltage. High leakage flux and lowering the main flux are disadvantages of having a short pole pitch. More voltage can be induced with the decrease in air gap length because of the decreased primary flux channel's reluctance and leakage while increasing the flux linkage [24].

Furthermore, the PMTFM is more reliant on the air gap as compared to PMRFM. For low power ratings in terms of bulk and cost, the air gap threshold should be smaller than 1 mm. Simulations of 8/16 PMTFG with double coil configuration are performed to test the effect of air gap diameter in PMTFG. Figure 14 shows PMTFG's influence of air gap diameter on back EMF.

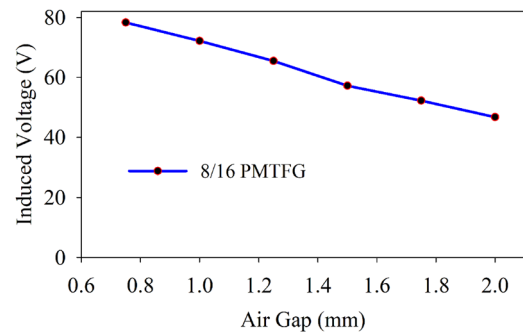


FIGURE 14 Induced voltage at different air gap lengths

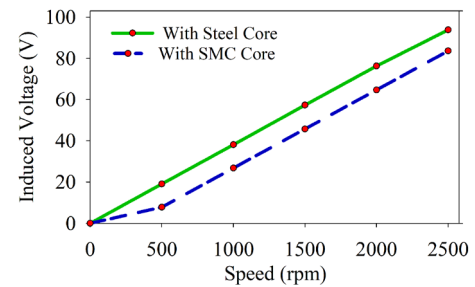


FIGURE 15 Induced voltage at different speeds of proposed design with both steel and SMC core

5.2 | Effect of stator core material

The continuous efforts to minimize energy consumption and increase the efficiency of electrical equipment play a major role in electrical machines with high efficiency. A thorough understanding of the magnetic material's properties is necessary for the design process. Different materials, such as silicon-iron (SiFe), nickel-iron (NiFe), and cobalt-iron (CoFe) lamination steels, as well as soft magnetic composites (SMC) and amorphous magnetic materials, are used for the core of machines [23].

Iron alloyed with a trace of silicon is the most commonly used material in electrical machines. The iron is chosen based on the core's permeability and the value of magnetic flux density at which saturation occurs in the iron. Furthermore, the magnetic losses in the rotor and stator cores are affected by material characteristics, lamination thickness, and the bonding of iron powder particles. A novel form of soft magnetic material is SMC, which has several advantages over traditional silicon steels, including magnetic and thermal isotropy and low eddy current losses; however, it has low permeability and poor mechanical performance [23]. Figure 15 shows the induced voltage at different speeds of efficient design with both steel and SMC core. Figures 16 and 17 show the efficiency versus output power and iron losses at different load values. The model with an SMC core has low iron losses compared to steel, which makes the design more efficient. According to the investigation, both machines yield similar results with minor changes. As a result, both alternatives are still being studied for PMTFM design.

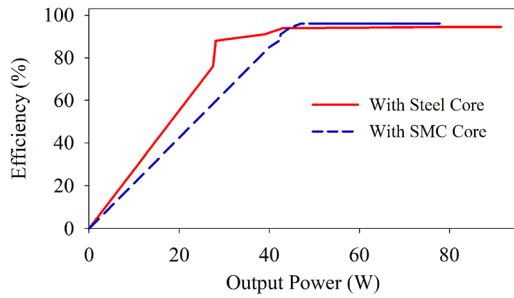


FIGURE 16 Efficiency versus output power of proposed design with both steel and SMC core

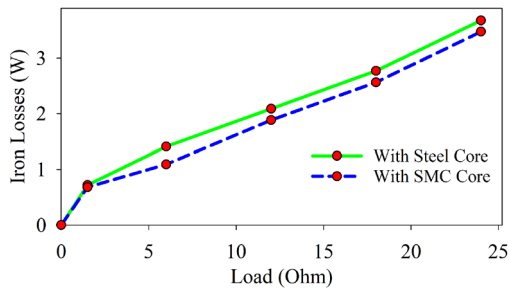


FIGURE 17 Iron losses at different loads of proposed design with both steel and SMC core

6 | PERFORMANCE COMPARISON

In comparison to the conventional PMTFG, the simulated PMTFG models include a few interesting features and shortcomings. All models are compared to each other and conventional model based on performance characteristics such as flux linkage, induced EMF, current, power, and efficiency. All the designed specifications are kept the same as standard PMTFG in order to make a valid comparison.

As previously stated, three designs with a single and double stator coil are simulated. The number of stator C-cores are reduced to 8 in 8/16 PMTFG, decreasing the stator mass, lowering iron losses, and thereby improving efficiency. In the subsections provided in Section 3, all performance parameters are compared. Considering flux linkage, back-EMF, and output power, the double coil 12/24 design yields superior performance. Furthermore, the efficiency and total power density of the 8/16 PMTFG with a double stator coil is higher.

Table 2 also shows that the 8/16 PMTFG has a total power density (TPD) that is 18% higher than the standard PMTFG and 4.5% higher in the case of the 10/20 PMTFG. More stator cores and rotor PMs mean more iron losses and weight for a 10/20 PMTFG compared to an 8/16 PMTFG with a double coil configuration. From Table 2, it is concluded that the double coil 8/16 PMTFG is an attractive option for fabrication because of its high performance, low cost, and simple design.

TABLE 2 Performance comparison of design models

Parameter	Conventional TFG	10/20 Double Coil PMTFG	8/16 Double Coil PMTFG
Number of C-cores	12	10	8
Rotor-PMs	24	20	16
Number of coils	01	02	02
Induced EMF	70.5V	76.3V	57.28V
Efficiency	86%	90.5%	94.5%
THD	3.9%	3.2%	3.0%
TPD (kW/kg)	0.0429	0.05086	0.0524

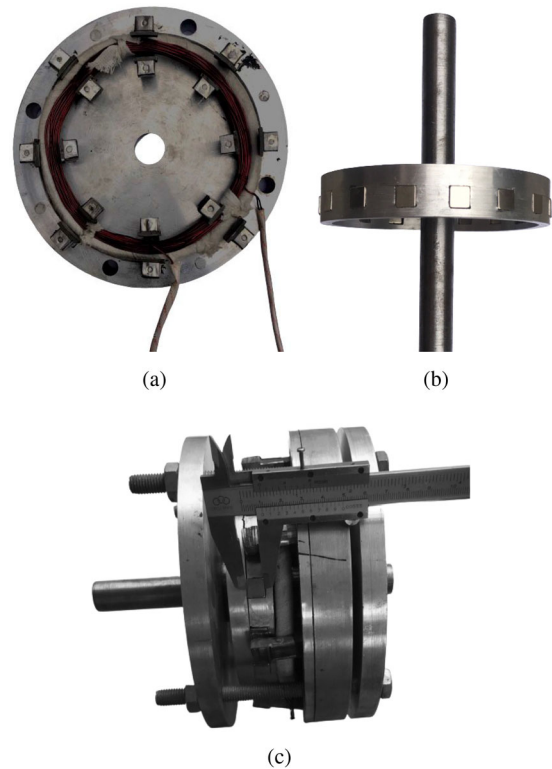


FIGURE 18 Hardware parts of the presented PMTFG: (a) whole stator in aluminium casing, (b) rotor, and (c) complete prototype

7 | PROTOTYPE TESTING

The single-phase, single-sided, double-coil 8/16 PMTFG is constructed and tested because it is the most efficient model of all the proposed designs. First, slots are cut into the stator housing made of aluminium to accommodate stator core segments. The proposed design uses a pole-shoe and a semi-closed C-core in the stator, which is different from the norm for PMTFG. As a result, unlike a standard PMTFG, installing the stator coil into the pole shoe can be a bit of a hassle. The cores are then inserted into the stator housing after the coils have been installed, as shown in Figure 18. Similarly, the neomax PMs in the PMTFG rotor design are housed in an aluminium housing. Figure 19 depicts the prototype's testing setup. The test

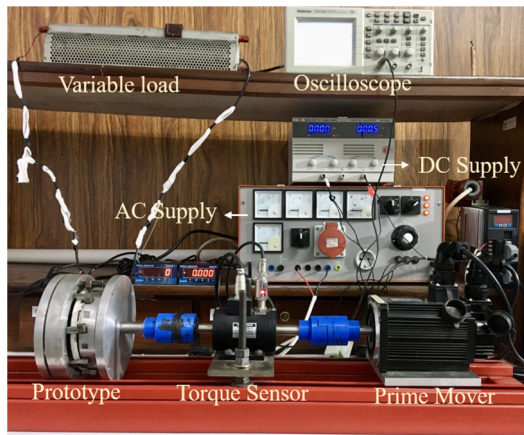


FIGURE 19 Test bench

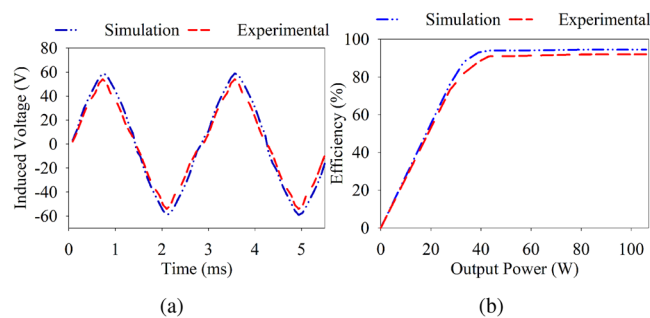


FIGURE 20 Comparison of FEM and experimental results of 8/16 PMTFG: (a) induced-EMF; (b) power versus efficiency

bench contain the prototype; a servo motor of 1.5 KW, 5 Nm and 6A; a torque sensor and variable load of 53 ohm with 5% tolerance. In Figure 20, FEA is used to generate the induced-EMF and output power versus efficiency of the 8/16 PMTFG, which is then compared to the measured data. The results of the simulation and the experiments appear to adapt to one another with the right amount of flexibility. The slight difference can be attributed primarily to the speed variation of the prime mover, which consists of a servo motor and its drive. Another contributor to the discrepancy between simulation and experiment is manufacturing tolerance. The 8/16 PMTFG had a power factor of 0.87 because only a variable resistive load was used to test the machine's efficiency.

8 | CONCLUSION

This paper presents the design and performance analysis of a new PMTFG having 8 stator C-cores and 16 rotor PMs. The proposed design's significant contribution is using a double coil in armature winding, a pole-shoe, and a simple design to minimize iron losses while providing high efficiency at a low cost. According to the core pole research, the double coil 8/16 PMTFG features the best flux linkage, improved back EMF, decreased weight, high power density, and efficiency. Load and no-load analyses are carried out to validate the effectiveness of

the proposed model. Additionally, 3D FEA was used to assess the flux linkage profile, no-load torque, induced voltage, load current concerning load voltage and efficiency, and load current versus power, which produced noticeably improved results. Further analyses were carried out to examine the performance of the proposed PMTFG, like the effect of stator core materials and air gap length. The suggested design has many benefits, such as a high power density, modular construction, easier winding, and the ability to handle faults.

AUTHOR CONTRIBUTIONS

Ali Muhammad: Conceptualization, methodology, software, validation, writing - original draft. Faisal Khan: Conceptualization, formal analysis, investigation, project administration, supervision. Basharat Ullah: Data curation, formal analysis, software, visualization, writing - review and editing. Ahmad Milyani: Formal analysis, funding acquisition, project administration, resources, visualization. Abdullah Azhari: Data curation, funding acquisition, project administration, visualization.

CONFLICT OF INTEREST

The authors have declared no conflict of interest.

FUNDING INFORMATION

None.

DATA AVAILABILITY STATEMENT

The data that supports the findings of this study are available on request from corresponding author.

ORCID

Basharat Ullah  <https://orcid.org/0000-0001-8201-602X>

REFERENCES

- Zheng, P., Zhao, Q., Bai, J., Yu, B., Song, Z., Shang, J.: Analysis and design of a transverse-flux dual rotor machine for power-split hybrid electric vehicle applications. *Energies* 6(12), 6548–6568 (2013)
- Ejlali, A., Soleimani, J., Vahedi, A.: Review in transverse flux permanent magnet generator design. *Iran. J. Electr. Electron. Eng.* 12(4), 257–269 (2016)
- Jia, Z., Lin, H., Fang, S., Huang, Y.: A novel transverse flux permanent magnet generator with double c-hoop stator and flux-concentrated rotor. *IEEE Trans. Magn.* 51(11), 1–4 (2015)
- Dobzhanskyi, O., Gouws, R.: Performance analysis of a permanent magnet transverse flux generator with double coil. *IEEE Trans. Magn.* 52(1), 1–11 (2015)
- Patel, M.A., Vora, S.C.: Analysis of a fall-back transverse-flux permanent-magnet generator. *IEEE Trans. Magn.* 53(11), 1–5 (2017)
- Lu, K., Wu, W.: High torque density transverse flux machine without the need to use SMC material for 3-D flux paths. *IEEE Trans. Magn.* 51(3), 1–4 (2015)
- Wan, Z., Husain, I.: Design, analysis and prototyping of a flux switching transverse flux machine with ferrite magnets. In: 2017 IEEE Energy Conversion Congress and Exposition (ECCE), pp. 1227–1233. IEEE, Piscataway, NJ (2017)
- Baker, N.J., Jordan, S.: Comparison of two transverse flux machines for an aerospace application. *IEEE Trans. Ind. Appl.* 54(6), 5783–5790 (2018)
- Jian, L., Gong, Y., Wei, J., Shi, Y., Shao, Z., Ching, T.: A novel claw pole memory machine for wide-speed-range applications. *J. Appl. Phys.* 117(17), 17A725 (2015)

10. Liu, C., Lu, J., Wang, Y., Lei, G., Zhu, J., Guo, Y.: Design issues for claw pole machines with soft magnetic composite cores. *Energies* 11(8), 1998 (2018)
11. Peng, G., Wei, J., Shi, Y., Shao, Z., Jian, L.: A novel transverse flux permanent magnet disk wind power generator with h-shaped stator cores. *Energies* 11(4), 810 (2018)
12. Zhao, X., Niu, S.: Design of a novel consequent-pole transverse-flux machine with improved permanent magnet utilization. *IEEE Trans. Magn.* 53(11), 1–5 (2017)
13. Kaiser, B., Parspour, N.: Transverse flux machine-a review. *IEEE Access* 10, 18395–18419 (2022)
14. Liu, C., Wang, X., Wang, Y., Lei, G., Guo, Y., Zhu, J.: Comparative study of rotor PM transverse flux machine and stator PM transverse flux machine with SMC cores. *Electr. Eng.* 104(3), 1153–1161 (2022)
15. Ueda, Y., Takahashi, H., Ogawa, A., Akiba, T., Yoshida, M.: Cogging-torque reduction of transverse-flux motor by skewing stator poles. *IEEE Trans. Magn.* 52(7), 1–4 (2016)
16. Ueda, Y., Takahashi, H.: Transverse-flux motor design with skewed and unequally distributed armature cores for reducing cogging torque. *IEEE Trans. Magn.* 53(11), 1–5 (2017)
17. Viktor, G., Dobzhanskyi, O., Rostislav, G., Gouws, R.: Improvement of transverse-flux machine characteristics by finding an optimal air-gap diameter and coil cross-section at the given magneto-motive force of the pms. *Energies* 14(3), 755 (2021)
18. Taravat, S., Kiyomarsi, A., Bracikowski, N.: Mitigation of cogging torque in transverse-flux permanent-magnet machines with flux concentrators by step skewing of stator pole. *IET Electr. Power Appl.* 14(12), 2378–2388 (2020)
19. Nasiri.ZARANDI, R., Toulabi, M.S., Shahnani, A.K.: Two-segment magnet transverse flux ferrite PM generator for direct-drive wind turbine applications: nonlinear 3-d mec modeling and experimental validation. *IEEE Trans. Energy Convers.* 37(3), 1834–1843 (2022)
20. Dobzhanskyi, O., Gouws, R., Amiri, E.: On the role of magnetic shunts for increasing performance of transverse flux machines. *IEEE Trans. Magn.* 53(2), 1–8 (2016)
21. Muhammad, A., Khan, F., Yousuf, M., Ullah, B.: Design and analysis of semi-closed stator core transverse flux permanent magnet generator. *World J. Eng.* (2021)
22. Pourmoosa, A.A., Mirsalim, M.: A transverse flux generator with a single row of permanent magnets: analytical design and performance evaluation. *IEEE Trans. Ind. Electron.* 66(1), 152–161 (2018)
23. Kumar, R., Zhu, Z.Q., Duke, A., Thomas, A., Clark, R., Azar, Z., et al.: a review on transverse flux permanent magnet machines for wind power applications. *IEEE Access* 8, 216543–216565 (2020)
24. Svehkarenko, D., Soulard, J., Sadarangani, C.: Analysis of a novel transverse flux generator in direct-driven wind turbines. In: *International Conference on Electrical Machines (ICEM)*, pp. 424–1. (2006)

How to cite this article: Muhammad, A., Khan, F., Ullah, B., Milyani, A.H., Azhari, A.A.: Design and FEM analysis of high-power density C-core permanent magnet transverse flux generator with reduced PM volume. *IET Renew. Power Gener.* 17, 885–893 (2023). <https://doi.org/10.1049/rpg2.12642>